

# Optimization of Production Parameters for Fabrication of Gum Arabic/Whey Protein-Based Walnut Oil Loaded Nanoparticles and Their Characterization

Ali Tahir, Rabia Shabir Ahmad,\* Muhammad Kamran Khan, Muhammad Imran, and Gebremichael Gebremedhin Hailu\*



Cite This: *ACS Omega* 2024, 9, 22839–22850

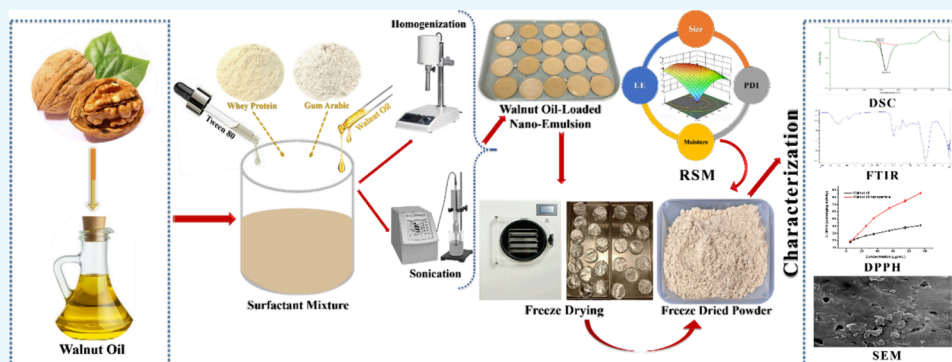


Read Online

ACCESS |

Metrics & More

Article Recommendations



**ABSTRACT:** The encapsulation of fatty acids, including walnut oil, within complexes is a promising strategy to address challenges, for instance, low water solubility and susceptibility to oxidation while incorporating these oils into food products. Additionally, encapsulation can effectively mask undesirable odor and flavor. The current study focuses on the optimization of walnut oil nanoparticles (WON) using complexes fabricated from gum arabic and whey protein by applying a response surface methodology. The impact of three different independent variables were determined, such as surfactant mixture (33–66%), walnut oil (5–25%), and sonication time (60–300 s), under three distinct desired conditions (low, medium, and high) on four different responses, i.e., particle size, polydispersity index (PDI), moisture level, and encapsulation efficiency (EE). The findings of the present study indicate that the point prediction-based WON resulted in significantly low particle size (82.94 nm), PDI (0.19), moisture content (3.49%), and high EE (77.26%). Fourier transform infrared spectroscopy (FTIR) study demonstrated the successful encapsulation of walnut oil and wall material into nanocapsules. Differential scanning calorimetry (DSC) verified the improved thermal stability property of WON after incorporation, and scanning electron microscopy (SEM) indicated that the WON had relatively fragile and smooth surfaces, along with the presence of few porous structures. The recorded experimental data from the existing study showed that the developed formulation of WON was potentially useful as a value-added ingredient for food industries.

## 1. INTRODUCTION

In previous decades, walnut oil has gained attention as a functional ingredient due to its high level of essential fatty acids and tocopherols, making it a valuable dietary source. Conspicuously, walnut oil triglycerides contain a significant proportion of polyunsaturated fatty acids (including linoleic and  $\alpha$ -linoleic acids) and monounsaturated (such as oleic acid).<sup>1</sup> In accordance with several studies, small quantities of bioactive compounds, including phytosterols and tocopherols are present in walnut oil.<sup>2</sup> Walnut oil contains significant amounts of polyunsaturated fatty acids, known to lower coronary heart disease risk. Additionally, the abundance of naturally occurring antioxidants in walnut oil provides protection against a lot of malignant conditions.<sup>3</sup> However,

the effective and practical inclusion of walnut oil into processed food products is minimal due to its high susceptibility to oxidation and low solubility.<sup>4</sup>

Similar to the case for other oils, two major challenges are encountered when walnut oil is incorporated into food products: First, walnut oil is hydrophobic in nature and does not readily dissolve in water, so preparing it as a micro/

Received: February 5, 2024

Revised: April 30, 2024

Accepted: May 10, 2024

Published: May 16, 2024



nanoemulsion facilitates oil particle dispersing easily in water.<sup>5</sup> The second challenge is associated with the inherent instability found in the structure of polyunsaturated fatty acids, rendering them prone to oxidative stress.<sup>6</sup> Furthermore, the unfavorable odor and flavors associated with walnut oil can lead to a decline in the overall quality and sensory attributes of food products.<sup>7,8</sup>

After many studies, it has been found that the only solution to resolve this problematic aspect is to apply the nanoencapsulation system because this advanced technology involves entrapping active ingredients/compounds into capsules with nanometer sizes. It proves effective and convenient in boosting the physical stability and provides a protective layer against reactions with other food components. The tiny size of these nanocapsules provides a pivotal role in augmenting the bioactivity of active materials, offering a practical solution to increase their overall efficacy.<sup>9</sup> Nanocapsules provide a protective barrier for core materials against unfavorable conditions, such as enzyme degradation, pH, and oxidation. Additionally, they can enhance the controlled release mechanism, providing further versatility in the application of this technology.<sup>10</sup> Whey protein is a great substitute for capsule walls due to its unique functional attributes. Whey protein is commonly employed as a coating material, owing to its biodegradability, safety, extensive availability, and continuous film-forming capabilities. Moreover, whey protein exhibits surface-active features, low oxygen permeability, and high tensile strength. These qualities make whey protein well-suited for the use of encapsulating coating materials, especially when combined with different polymeric substances. This combination proves beneficial for target delivery and enhanced stability of encapsulated formulations.<sup>11</sup> Whey proteins have the ability to bind the hydrophobic ligands, such as retinol, hydrophobic peptides, chromatographic phases with hydrophobic properties, melittin from oleic acid, and apitoxin.<sup>12</sup>

Gum arabic plays a pivotal role as a core material in the nanoencapsulation of flavor compounds. Its noteworthy characteristics, such as favorable solubility, emulsifying properties, low viscosity, and a high holding capacity of oil droplets and volatile compounds, have garnered significant attention in the field of nanoencapsulation.<sup>13</sup> Proteins like whey, soy protein isolates, and sodium caseinate serve as common wall materials in nanoencapsulation, leveraging their diverse functional groups, amphiphilic characteristics, self-assembly capabilities, and substantial molecular weight to achieve desired functional properties, i.e., viscosity, layer-forming ability, solubility, and emulsifying capacity.<sup>14</sup> A combination of plant- and animal-based protein blends provides additional advantages regarding continuous film creation, stability, biodegradability, emulsification, and extensive structural qualities. These specific types of blends exploit the strengths of both sources to enhance the overall effectiveness of the proteins in various concentrations.<sup>15</sup> However, no direct comparison of these two types of wall materials with walnut oil has been performed yet, and the behavior of these encapsulated in food products remains unknown.

Response surface methodology (RSM) comprises a set of statistical approaches that provide a solution for developing an optimal formulation and is contemplated as a more cost-effective methodology compared with other traditional processes of optimized formulation.<sup>16</sup> To build models and tests, the RSM technique included a factorial design and multiple regression analysis. Furthermore, the RSM was used

to assess the individual effects of each processing parameter on total efficiency. The Box–Behnken design (BBD) served as a standard experimental framework design tool, offering numerous advantages such as fewer experiments and shorter periods compared to other methods for analyzing and identifying multiple factors and relationships amid independent variables.<sup>17</sup> Several investigators have proposed that RSM is an effective method for optimizing conditions for nanoencapsulation systems. In accordance with Saravana, Shanmugapriya, Gereniu, Chae, Kang, Woo, and Chun,<sup>18</sup> RSM is an excellent method that can describe the optimal influence of sonication parameters on fucoxanthin oil-based nanoencapsulation with appropriate size, zeta potential, along with good polydispersity range. In the study undertaken by Yang, He, Ismail, Hu, and Guo,<sup>19</sup> the formulation of a thyme essential oil-based nanoemulsion was optimized using the ultrasonication method through the RSM. This approach could give the ideal time and power of the sonication system, as well as emulsifier concentration to produce a nanoemulsion with optimal size, polydispersity, and zeta potential, with a minimum inhibitory and bactericidal concentration.

The present study's first aim is to employ RSM (BBD) for encapsulating walnut oil (O/W) through a constant biopolymeric system via soluble complexation procedure sonication and freeze-drying. RSM tool was used to explore the relationship of different independent variables along with surfactant mixture (gum arabic/whey protein, walnut oil, and sonication time on the particle size, polydispersity index (PDI), moisture content, and encapsulation efficiency (EE) of encapsulated walnut oil loaded nanoparticles (WON)). The second and most important goal of this research was to inspect the attributes of the WON formulations/powder to recognize whether it meets the requirements for future food product development or not. The third aim was to assess the chemical composition of the WON and morphological characteristics. If successful and efficient nanoencapsulation can be achieved, then these WONs may be appreciated as a part of value-added food products within the food processing industry. It must be highlighted that the novelty of the present research lies in applying gum arabic/whey protein formulations (complexes) for entrapping walnut oil and the subsequent formation of nanocarriers utilizing these complex formulations.

## 2. MATERIALS AND METHODS

**2.1. Materials.** Walnut oil was procured from fresh vintage forms. Whey protein was bought from GNC Super Foods, USA, and gum arabic was obtained from BioChem, USA. Tween 80 and other high-purity chemical materials were purchased from Sigma-Aldrich (USA).

**2.2. Preparation of WON.** Stock solutions of wall material were prepared by applying a gum arabic and whey protein mixture by using distilled water. To achieve complete dissolution and thorough rehydration, the samples were positioned in a water bath (IKA, HB-4, Germany) for 12 h at 70 °C. The wall materials ratio (gum arabic/whey protein) for complex formation was set at 1:1, 1:2, and 2:1, as indicated in Table 1. Maintaining a consistent concentration of 30% w/v total soluble solids, walnut oil specified in Table 1 was introduced into the surfactant mixture/wall material solutions, along with Tween 80 as an emulsifier. It improves the solubility of hydrophobic compounds and enhances the bioavailability of encapsulated materials. The developed mixture was continuously stirred at 65 °C by using a magnetic stirrer (LS-100,

**Table 1. BBD-Based WON Formulations and Their Levels**

	symbol	coded values		
		low-level (−1)	mid-level (0)	high-level (+1)
Independent Variable				
A = surfactant mixture	%	33	49.5	66
B = walnut oil	%	5	15	25
C = sonication time	s	60	180	300
Dependent Variable				
W <sub>1</sub> = particle size	nm		low	
W <sub>2</sub> = polydispersity	mean		low	
W <sub>3</sub> = moisture content	%		low	
W <sub>4</sub> = encapsulation efficiency	%		high	

LabTron, Iran). The pH of the surfactant mixtures was set at 7.00 through NaOH (1 M) by taking care of the isoelectric point of whey protein to form soluble complexes.

Subsequently, a rotor-stator homogenizer (Wise, 15D, South Korea) was used to homogenize the prepared samples by running at 10000 rpm for 10 min. These formulations were subjected to a sonication process at a given time (1 s on and 1 s off), (Table 1). For the sonication purpose, a probe sonicator (Heischler, UPS-200, Germany) was used with a 20 kHz frequency limit and 80% full power at 25 °C before the annealing step. Finally, the prepared complexes were frozen overnight at −20 °C and then subjected to freeze-drying (8624-FDU, Operon, South Korea) for 48 h at −85 °C. The resulting samples were converted carefully into powder form using a grinder and reserved in the plastic tubes until further analysis.<sup>20</sup>

**2.3. BBD Optimization.** The integration of optimization approaches in formulating materials through experimental design has become a standard practice. While there are various designs of experiment techniques reported for optimization, the BBD was specifically preferred among them for its efficiency, requiring fewer experimental runs than other designs.<sup>21</sup> Numerous experimental studies on a wide range of nanosized formulations have been reported, demonstrating the

effectiveness of this approach in the development of optimal formulations.<sup>22,23</sup> A three-level/factor BBD method was applied to obtain optimized WON, by considering three different independent variables with the ranges of surfactant mixture (A; 33–66%), walnut oil concentration (B; 5–25%), and sonication time (C; 60–300 s), and dependent variables (particle size, polydispersity, moisture, and encapsulation efficiency (Table 1)). Seventeen experimental compositions (WON), incorporating the dependent variables at low, medium, and high levels, are detailed in Table 2. The 3D surface plot illustrates the relationship of each variable on the response assessment. Ultimately, the optimized parameters and their corresponding response values were determined. Optimized WON was selected based on minimum particle size, polydispersity, and moisture content, and high encapsulation efficiency by the point prediction method. The quadratic polynomial model is represented through the given equation below:

$$W = \beta_0 + \sum_{i=1}^3 \beta_i X_i + \sum_{i=1}^3 \beta_{ii} X_{ij} + \sum_{i<j}^3 \beta_{ij} X_i X_j \quad (1)$$

W represents the independent variables for the dependent responses (A–C); and  $\beta_0$  denotes the intercept  $\beta_i$ ,  $\beta_{ii}$ , and  $\beta_{ij}$  denote the linear, quadratic, and interaction model coefficient terms, respectively. In contrast,  $X_i$  and  $X_j$  denote the independent factors.

**2.4. Particle Size and PDI.** The dynamic light scattering (Zetasizer, Malvern Instruments, UK) method was employed to calculate both the size and PDI of the developed WONs by diluting samples into 100 mL of double distilled water. A PDI below 0.1 suggests a homogeneous/uniform population, whereas a PDI exceeding 0.3 indicates significant heterogeneity between particles.

**2.5. Moisture Content.** Briefly, 5 g of WON sample was dried in the oven (400-UFB, Memmert, Germany) at 105 °C for 24 h. The quantification of the moisture level involved measuring the weight variation before and after the drying procedure.

**Table 2. BBD Plan for WON with Independent and Dependent Variables**

run	independent variables			dependent variables							
	A (%)	B (%)	C (Sec)	particle size (nm)		polydispersity (mean)		moisture content (%)		encapsulation efficiency (%)	
				experimental	predicted	experimental	predicted	experimental	predicted	experimental	predicted
1	66	5	180	113.24	113.04	0.35	0.33	5.97	5.61	71.09	72.17
2	33	15	300	117.31	114.79	0.18	0.20	4.22	3.99	69.48	71.07
3	66	15	300	97.56	99.68	0.32	0.33	5.53	5.34	71.55	71.62
4	49.5	25	300	94.74	97.06	0.38	0.34	4.18	4.04	74.91	74.41
5	49.5	15	180	85.34	82.94	0.18	0.19	3.69	3.49	78.02	77.27
6	33	25	180	114.45	114.65	0.30	0.31	4.65	5.01	76.61	75.53
7	33	15	60	111.56	109.44	0.35	0.34	5.67	5.86	72.15	72.08
8	49.5	15	180	80.18	82.94	0.18	0.19	3.69	3.49	74.26	77.27
9	49.5	5	60	107.54	105.22	0.33	0.36	5.02	5.16	71.01	71.52
10	49.5	5	300	116.67	114.75	0.28	0.28	3.87	4.42	72.73	71.58
11	49.5	15	180	82.36	82.94	0.18	0.19	3.65	3.49	77.98	77.27
12	49.5	15	180	85.41	82.94	0.17	0.19	3.41	3.49	78.03	77.27
13	66	15	60	109.12	111.65	0.31	0.28	4.76	4.99	71.22	69.63
14	33	5	180	95.74	100.19	0.27	0.24	4.98	4.65	69.76	69.32
15	49.5	25	60	111.30	113.22	0.36	0.35	5.37	4.82	72.34	73.49
16	49.5	15	180	81.41	82.94	0.24	0.19	3.01	3.49	78.04	77.27
17	66	25	180	93.34	88.90	0.27	0.29	4.21	4.53	70.34	70.78

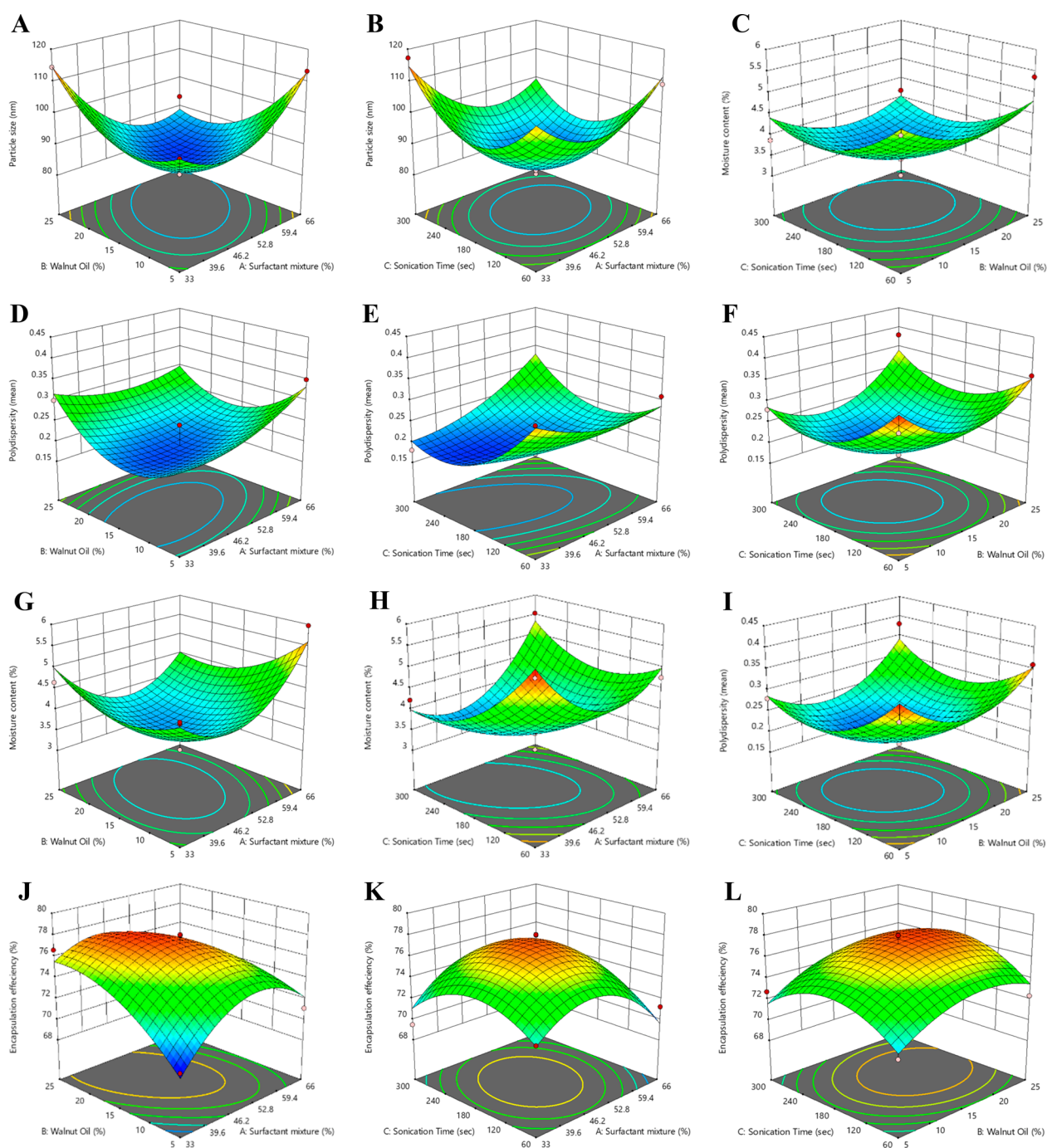


**Figure 1.** Three-dimensional (3D) response surface plots of walnut oil nanoparticles on particle size (A–C), polydispersity (D–F), moisture content (G–I), and encapsulation efficiency (I, J).

**2.6. Encapsulation Efficiency (EE).** Powder-free surface walnut oil was intricately blended with 2 mL of distilled water and vigorously shaken for a duration of 1 min. Following this, the solution underwent a meticulous extraction process utilizing a 25 mL combination of hexane and isopropanol in a 1:3 ratio, followed by centrifugation at 4000 rpm for a duration of 20 min. The distinct organic phase was carefully isolated, and the aqueous phases underwent an additional round of extraction. The resulting solution, enriched with encapsulated oil (WON), underwent a drying process at 105 °C, and the residual oil content was precisely measured.<sup>20</sup>

For the comprehensive extraction of total oil, 2.5 mL of distilled water was mixed with 0.6 g of WON, and the mixture was efficiently vortexed for 2 min. The overall process for the extraction of total oil mirrored that of the encapsulated oil. The EE was accurately measured utilizing the formula given below:

$$EE = \frac{\text{Encapsulated oil (g/100 g powder)}}{\text{Total oil (g/100 g powder)}}$$

**2.7. Antioxidant Activity.** The assessment of antioxidant properties in walnut oil and the WON was conducted using the 1,1-diphenylpicrylhydrazyl (DPPH) method, following the methodology outlined by Sharma and Bhat.<sup>24</sup> For the

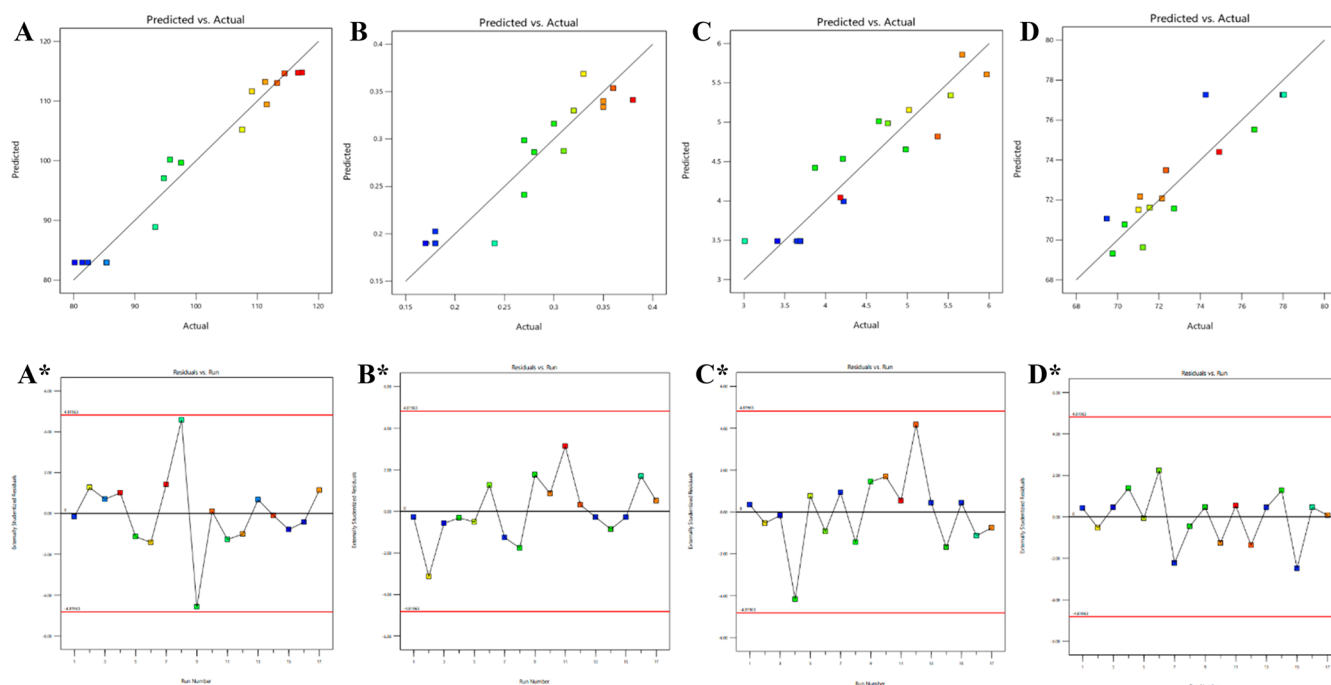


**Figure 2.** Linear correlation plots (A–D) between observed and predicted values of the responses (particle size, polydispersity, moisture content, and encapsulation efficiency) and their corresponding plots of residual versus run (A\*, B\*, C\*, and D\*).

examination of WON, a solution with a concentration of 1 mg/mL was further diluted to varying absolute concentrations (5, 10, 15, 25, 35, 45, 65, 85, and 100  $\mu\text{g}/\text{mL}$ ) in water. Following this, 300  $\mu\text{L}$  of a methanolic DPPH solution (1 mL, 0.3 mmol) was introduced to both WO and WON. The resulting mixture was subjected to a 30 min incubation at 25  $^{\circ}\text{C}$  under a dark environment, and then absorbance was meticulously recorded at a wavelength of 517 nm using the accuracy of a UV–vis-1800 spectrophotometer. To quantify the final scavenging activity, a scrupulous formula was employed, allowing for the precise determination of the antioxidant level of the primed mixture. This approach ensures an accurate and reliable assessment of the scavenging activity of the solution under investigation.

$$\text{Scavenging activity \%} = A_{\text{Control}} - A_{\text{Sample}}/A_{\text{Control}} \times 100$$

### 2.8. Fourier Transform Infrared Spectroscopy (FTIR).

FTIR spectra were acquired with a Nicolet iS10-spectrometer (Thermo-Fisher Scientific, USA). Concisely, freeze-dried WON was taken and mixed with KBr pellet and subsequently subjected to scanning within the range of 4000–400  $\text{cm}^{-1}$ , selecting a resolution of 4  $\text{cm}^{-1}$  to confirm the structure of whey protein-gum arabic walnut oil complexes/WON.<sup>25</sup>

**2.9. Differential Scanning Calorimetry (DSC).** DSC study was conducted on WON by employing a state-of-the-art differential scanning calorimeter (Q2000, TA INST., New Castle, DE). Freeze-dried WON powder was taped up in a small aluminum pan with the help of a presser (TZERO Press) and scanned under the range of 20–350  $^{\circ}\text{C}$  at a 10  $^{\circ}\text{C min}^{-1}$  heating rate. A reference unfilled pan was employed, and a one min equilibration at 0  $^{\circ}\text{C}$  was carried out prior to each run. The inert nitrogen gas was introduced by a flow rate of 20 mL/min throughout the experiment. 10 mg of WON powder was taped into pans with a capacity of 30  $\mu\text{L}$ . The protein denaturation kinetics were measured using residual denaturation enthalpy ( $\Delta H$ ) (J/g).<sup>26,27</sup> The final area was obtained

using Universal Analysis 2000 software from TA INST (Waters LLC, New Castle, DE).

**2.10. Scanning Electron Microscopy (SEM).** The morphological parameters of WON were studied through a SEM (8020-SU, Hitachi, Japan) and the magnification of 5–25000 $\times$  under high vacuum and 26 kV voltage.

**2.11. Statistical Analysis.** The experimental trials were accurately conducted in triplicate to ensure the robustness and reliability of the data. To scrutinize the statistical significance, analysis of variance (ANOVA) was applied with a significance level of  $P < 0.05$ . An in-depth exploration of mean differences among the experimental groups was then conducted through the utilization of Duncan's multiple-range test. To further enhance the precision of the study, advanced statistical techniques, namely, BBD, were implemented. This strategic approach not only allowed for the exploration of complex relationships between multiple variables but also facilitated the optimization of the experimental conditions. The entire statistical analysis, including the execution of BBD, was seamlessly carried out using the Design-Expert software (Windows version 13). Principal component analysis (PCA) was employed to offer a comprehensive overview of the relationships among various dependent responses, utilizing Minitab Statistical Software 19.

## 3. RESULTS AND DISCUSSION

**3.1. Response Surface Model Fitting.** Three levels per factor-based BBD tool were used to achieve the optimized WON. This design exhibited 17 formulations including three replicated points, as outlined in Table 2. The quadratic model appeared as the most fitting choice for measuring the intricacies of all responses under consideration. In order to provide a comprehensive visual representation of how independent variables influence each of the three responses, three-dimensional (3D) plots were accurately generated. These graphical representations, shown in Figure 1, offer vivid insight

into the intricate relationships and dynamics shaping the experimental outcomes. Figure 2A–D show linear correlation graphs illustrating the relationship of observed and predicted values for the respective responses. Additionally, corresponding residual versus run plots (Figure 2A\*–D\*) are presented. The ranges of experimental values for the observed responses, particle size (80.18–117.31 nm), PDI (0.17–0.38%), moisture content (3.01–5.97%), and EE (69.48–78.04%) were found to be incredibly closest to the predicted values (Table 2).

ANOVA presented a significant ( $P < 0.05$ ) model exhibiting a nonsignificant lack of fit. As presented in Table 3, the lack of

**Table 3. Results of Regression Coefficients and Analysis of Variance for Four Response Variables**

source	DF	$W_1$ : particle size	$W_2$ : polydispersity	$W_3$ : moisture content	$W_4$ : encapsulation efficiency
		estimated coefficient	estimated coefficient	estimated coefficient	estimated coefficient
intercept ( $\beta_0$ )	1	82.94	0.19	3.49	77.27
linear terms					
A ( $\beta_1$ )	1	-3.23	0.01	0.11	-0.47
B ( $\beta_2$ )	1	-2.42	0.01	-0.17	1.20
C ( $\beta_3$ )	1	-1.66	-0.02	-0.37	0.24
interaction terms					
AB ( $\beta_1\beta_2$ )	1	-9.65	-0.02	-0.35	-1.90
AC ( $\beta_1\beta_3$ )	1	-4.33	0.04	0.55	0.75
BC ( $\beta_2\beta_3$ )	1	-6.42	0.01	-0.01	0.21
quadratic terms					
$A^2$ ( $\beta_{11}$ )	1	11.29	0.03	0.94	-3.48
$B^2$ ( $\beta_{22}$ )	1	9.96	0.07	0.51	-1.83
$C^2$ ( $\beta_{33}$ )	1	14.66	0.07	0.60	-2.68
lack of fit	3	0.0823	0.1809	0.0762	0.3915
$P$ value		0.0003	0.0135	0.0234	0.0257
$F$ value		21.68	6.04	4.94	4.77
$R^2$		0.9654	0.8859	0.8640	0.8599
adj. $R^2$		0.9208	0.7392	0.6891	0.6797

fit was 0.0823, 0.1809, 0.0762, and 0.3915 for each model (particle size, PDI, moisture content, and EE, respectively). The resulting outcomes suggest that the model is valid and fits well. Based on the analysis of variance (ANOVA), the calculated  $F$ -values for all response variables were found to fall within the range of 4.77 to 21.68. To gauge the model's appropriateness, the desired coefficient of determination ( $R^2$ ) was set at 80%, indicating a well-fitted model. The current experimental design study utilizing BBD showcased higher  $R^2$  values, affirming its superior fit compared to alternative models. An effective statistical model is characterized by a minimal difference between  $R^2$  and adjusted  $R^2$ . Notably, in this study, marginal differences were observed between  $R^2$  and adjusted  $R^2$  for particle size (0.9654 and 0.9208), PDI (0.8859 and 0.7392), moisture content (0.8640 and 0.6891), and EE (0.8599 and 0.6797). These values, each hovering around 1,

suggest a robust correlation between the predicted outcomes and the experimental data, underscoring the accuracy and reliability of the established statistical model. The developed model demonstrated statistical significance, indicating a reliable relationship between the predicted and observed results.<sup>28,29</sup>

**3.1.1. Effect of Independent Variables on Particle Size.** The small sizes of intricate particles have a vital role in ensuring the stability of the encapsulation system against precipitation/creaming, making them well-suited for the food sector. Particle size and distribution significantly affect various physical attributes, including turbidity, stability, and rheological characteristics in colloidal systems.<sup>30</sup> The particle size of the encapsulated complexes is influenced by various factors. This study specifically investigated the effects of surfactant mixture, walnut oil concentration, and sonication time on WON particle size. Figure 1A–C provides a comprehensive representation of both the single and combined influences of the specified independent variables on the size ( $W_1$ ). Increasing surfactant concentration leads to a reduction in size, attributed to diminished interfacial tension between the lipid and aqueous phases. Consequently, this phenomenon encourages the development of emulsion droplets characterized by smaller particles.<sup>31</sup> An increased concentration of the surfactant mixture sustained the nanoparticles by creating a stearic boundary on the developed particle surface. This protective barrier prevented the particles from coalescing into larger ones.<sup>32</sup> A surfactant mixture helps to reduce the surface tension between liquids or between a liquid and a solid. It makes it easier for substances to mix and spread out. Adding a surfactant mixture above the optimum point can cause an increase in the particle size. This happens because the excess surfactant molecules start to form larger aggregates, which, in turn, leads to larger particle sizes. The excess surfactant molecules start to clump together, causing the particles to become bigger. Change in the oil concentration influences the size of the nanoparticle formulation. Higher oil concentrations result in reduced particle size due to a reduction in the internal phase viscosity. Additionally, a high sonication time continuously reduces the particle size, as prolonged sonication enables particle breakdown. Therefore, an intermediate sonication time is considered optimal for achieving the desired particle size range.

Masarudin, Cutts, Evison, Phillips, and Pigram<sup>33</sup> identified substantial intermolecular cross-linkage between anionic groups of whey protein and free primary amino group in gum arabic as pivotal for achieving a uniform particle size distribution. This cross-linking forms an intricate network that facilitates the consistent and controlled development of the nanoparticles. The development and stability of these nanoparticles in solution are intricately linked to the structural characteristics of various molecules in the sample. These interactions, particularly electrostatic ones, play a significant role, as highlighted by Stoylov,<sup>34</sup> emphasizing the importance of understanding these molecular dynamics in the context of nanoparticle formation and solution stability. The particle size range observed in all 17 developed formulations was between 80.18 to 117.31 nm, a range well-suited for topical delivery. These results align with those of Esfahani, Jafari, Jafarpour, and Dehnad,<sup>20</sup> where the smallest particle size range of gum arabic–gelatin formulations with fish oil/omega-3 ( $\omega$ 3) fatty acids nanocapsules was 26–114 nm.

$$W_1 \text{ (Particle Size)} = +82.94 - 3.23A - 2.42B - 1.66C \\ - 9.65AB - 4.33AC - 6.42BC + 11.29A^2 + 9.96B^2 \\ + 14.66C^2 \quad (2)$$

### 3.1.2. Effect of Independent Variables on Polydispersity.

The PDI was employed to assess the size distribution, and WON samples exhibited PDI values within acceptable limits. The PDI with a scale from 0 to 1, functions as an indicator of the uniformity of dispersion. A lower PDI value signifies a homogeneous population, while a high value points out increased heterogeneity.<sup>35</sup> The results obtained from the current investigations highlight the PDI of 17 samples, demonstrating a range between 0.17 and 0.38 ( $W_2$ ). These findings echo the observations made by Ali, Ali, Aqil, Imam, Ahad, and Qadir,<sup>21</sup> specifically in their examination of thymoquinone-loaded nanoparticles, where the PDI was reported to be under 0.19–0.29. The significant variability in the PDI values across the samples can be attributed to the multifaceted impact of diverse independent variables incorporated into the formulations. It is noteworthy that the interaction relationship of these independent variables on the PDI was explicitly illustrated through the utilization of 3D graphs, as depicted in Figure 1D–F. This graphical representation provides visual insight into how alterations in formulation variables contribute to variations in PDI, underlining the intricate nature of these relationships within the context of the study.

An increase in surfactant mixture and sonication time led to a positive variation in PDI, with sonication time signifying a less significant effect compared to the walnut oil amount. As sonication time increased, there was a corresponding rise in PDI, potentially due to nonuniform particle size reduction or few particle growths. Higher surfactant concentration resulted in an elevated PDI, possibly due to the formation and stabilization of smaller particles.

$$W_2 \text{ (Polydispersity)} = +0.19 + 0.01A + 0.01B - 0.02C \\ - 0.02AB + 0.04AC + 0.01BC + 0.03A^2 + 0.07B^2 \\ + 0.07C^2 \quad (3)$$

### 3.1.3. Effect of Independent Variables on Moisture.

In order to measure the stability of dried powder, the moisture content is an essential factor. The occurrence of high moisture in a product leads to particle agglomeration, which increases microbial growth, as well as oxidation.<sup>36</sup> Usually, the persistent amount of moisture in products can be controlled by adjusting the duration of the second drying stage. Several studies explore the drying processes of nanocapsules/nanoparticles using freeze-drying techniques.<sup>37</sup> Freeze-drying assists as a highly stable and secure method for enhancing the physicochemical stability of particles, particularly under challenging storage conditions of storage. Table 2 signifies the moisture level of produced WON-formulated powders, which is in the range of 3.01–5.97%, and 3D graphs (Figure 1G–I) show the relationship between independent variables and moisture content. Generally, particle size is significantly reduced by increasing the percentage of gum arabic because this occurrence can be attributed to the water-absorbing nature of hydrocolloids, for instance, gum arabic, which facilitates moisture retention in the samples. Consequently, formulations with higher concentrations of gum arabic had a higher moisture content compared to those with a higher proportion

of whey protein. The fluctuation in moisture level can be elucidated by considering the difference of water-binding groups in whey protein and gum arabic.

According to Vahidmoghdam, Pourahmad, Mortazavi, Davoodi, and Azizinezhad,<sup>14</sup> when entirely employing gum arabic as the wall material, there was an observable rise in moisture content as the concentration of the wall material decreased. This trend is likely endorsed by the ability of hydrocolloids to enhance the water-bonding capacity by sustaining and increasing the overall moisture level. This may clarify that the increased moisture in the gum arabic formulations compared with those containing whey protein could be due to inherent differences in the water-retaining properties between these two coating materials. As expected, the increase in water absorption can be associated with the hydrophilic nature of the hydrocolloid biopolymer. This property is likely the primary factor explaining a higher trend of moisture content observed in WON formulations with a ratio of 2:1 (gum arabic/whey protein).<sup>38</sup>

$$W_3 \text{ (Moisture content)} = +3.49 + 0.11A - 0.17B \\ - 0.37C - 0.35AB + 0.55AC - 0.01BC + 0.94A^2 \\ + 0.51B^2 + 0.60C^2 \quad (4)$$

### 3.1.4. Effect of Independent Variables on Encapsulation Efficiency.

The independent variables revealed their influence on the EE of WON, resulting in a range of 69.48% to 78.04% (Table 2) as well as the relationship between independent variables and EE ( $W_4$ ) was presented through the 3D graphs (Figure 1J–L). Reportedly, the EE of WON rises alongside an increase in the oil concentration percentage. The EE rises by an increase in the percentage of liquid lipids to solid lipids, potentially altering the crystal order of the lipid blend. The gradual infusion of more free oil into the coating material results in an elevation of EE. Conversely, saturating the wall materials by incorporating an excessive amount of oil may lead to a decline in nanocapsule EE. This observed pattern corresponds to the findings reported in various studies.<sup>21</sup>

The ratio of the surfactant mixture has also a significant effect on the EE of WON, as a gradual decrease in the EE was noted by an increase in the amount of surfactant mixture. The partition phenomenon could explain the decreasing trend in EE, as a higher percentage of surfactant mixture in the external phase increases the partition of the core material from an internal to the outer phase of the medium.<sup>21</sup> The inclusion of a high amount of chitosan and cinnamon oil in the solution increased with higher concentrations of the coating material in addition to enhancing the linkage between chitosan molecules.<sup>27</sup> However, the greater amount of chitosan led to a reduction in the amount of chitosan embedded in the cinnamon oil. The higher amount of cinnamon oil adheres to the surface of cinnamon oil nanoparticles, decreasing the microcapsules' surface charges.<sup>39</sup>

$$W_4 \text{ (Encapsulation efficiency)} \\ = +77.27 - 0.47A + 1.20B + 0.24C - 1.90AB \\ + 0.75AC + 0.21BC - 3.48A^2 - 1.83B^2 - 2.68C^2 \quad (5)$$

**3.1.5. Verification of the Optimized Model.** The response of all WON formulations was well suited to diverse kinetic sequences, and the optimal fitting design for the produced formulations was discovered to be a quadratic model. The

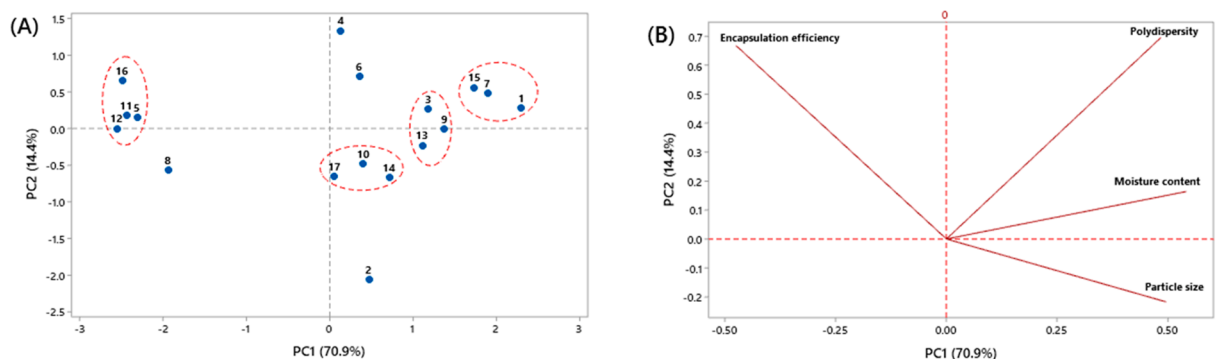


**Figure 3.** Principle component analysis (PCA) of walnut oil nanoencapsulation (A) score plot by different experimental attributes; (B) loading plot on particle size, polydispersity, moisture content, and encapsulation efficiency.

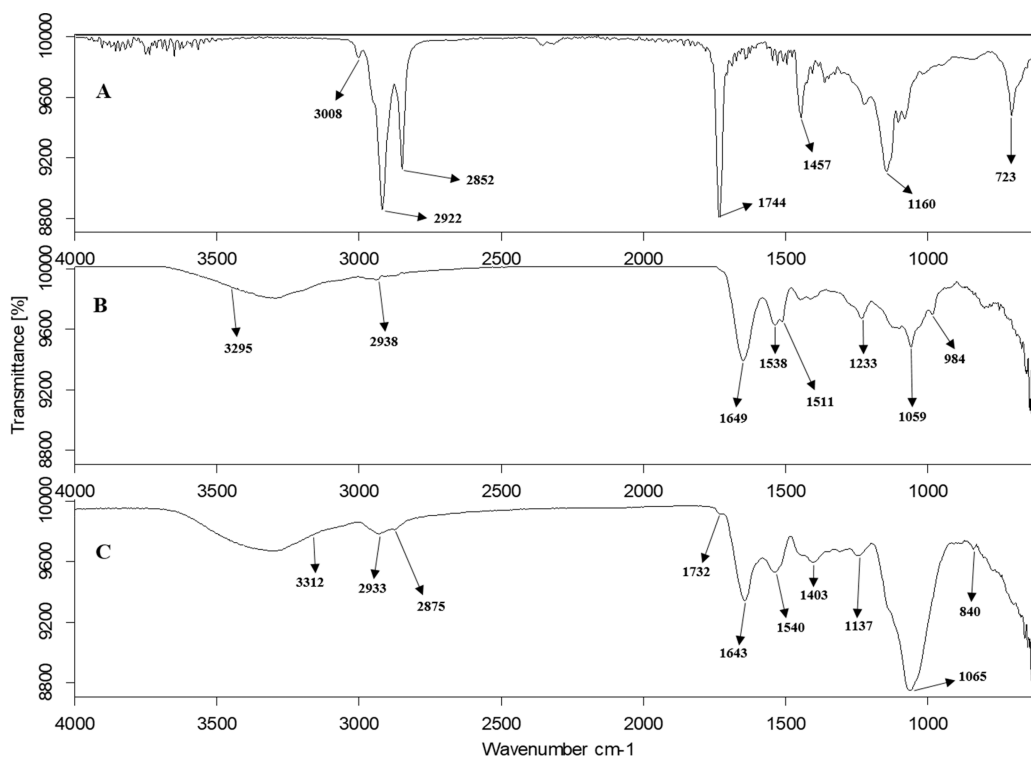


**Figure 4.** FTIR spectra of (A) walnut oil; (B) encapsulation wall material gum arabic + whey protein; (C) encapsulated walnut oil.

selection of the quadratic design is particularly favorable for WON formulations because each independent variable, both individually and in combination, exerts a significant influence on the dependent variables. The obtained experimental outcomes closely aligned with the predicted values obtained by the software, exhibiting a linear correlation. The optimized WON was selected based on the standards of achieving the minimal particle size, PDI, and moisture along with the highest EE value by selecting the point prediction technique. The WON conformation was found to meet the requirements of an optimum design with a surfactant mixture (49.50%), walnut oil (15%), and a sonication time (180 s). The optimized WON sample has a particle size of 82.94 nm and zeta potential of  $-4.03$  mV with PDI, moisture, and EE 0.19 mean, 3.49%, and 77.26% respectively. Based on the BBD design, the optimized WON samples were selected and stored for analysis and further characterization.

**3.2. Principal Component Analysis (PCA).** Principal component analysis (PCA) was employed to succinctly

summarize and visually represent various dependent variables including particle size, polydispersity, moisture content, and encapsulation efficiency, in order to identify patterns among 17 runs. PCA, known for its efficacy in minimizing the resulting multidimensional data to two or more components, ensures limited deprivation of experimental details.<sup>40</sup> Figure 3A illustrates the positions of the working treatments, while the spatial distribution of quality attributes within the space defined by the PC-1 and PC-2 dimensions is depicted in Figure 3B. The original variance of variables by PC1 and PC2 accounted for 70.9% and 14.4%, respectively (Figure 3). The sum of both principal components explained 85.3% of the variations among the variables.

Samples 1, 7, and 15 were positioned in the same quadrant on the positive side of both PC-1 and PC-2. This positioning implies a minimally significant difference between these formulations and suggests relatively higher values for the variables under consideration. In the score plot, three groups were classified for PC-1 versus PC-2, meaning that the ratio of

the surfactant mixture and walnut oil and sonication time critically affected the walnut oil formulations, whereas sample 10 is situated in the same quadrant and in close proximity to samples 14 and 17, indicating the least significant difference among these samples. Furthermore, samples 3, 9, and 13 were found in close proximity, which shows the similarity among these samples in the score plot diagram. The similarity among these samples (3, 9, and 13) is due to the EE and PDI, which are very close to each other. In addition to this, an analogous to the relationship was observed among samples 5, 11, 12, and 16 (Figure 3A). As presented in Figure 3B, PC-1 was positively correlated with particle size, polydispersity, and moisture content but negatively related to encapsulation efficiency, while PC-2 was positively related to polydispersity, moisture content, encapsulation efficiency, and negatively related particle size. Consequently, PCA proves to be a well-suited chemometric tool to deliver statistics on classification among samples of WON and correlation with particle size, polydispersity, moisture content, and encapsulation efficiency.

**3.3. Structural and Thermal Stability.** FTIR was used to investigate the secondary structure of encapsulated walnut oil in the whey protein and gum arabic mixture. As shown in Figure 4, the spectrum of pure walnut oil exhibited band at  $3008\text{ cm}^{-1}$  due to the stretching vibrations of  $-\text{OH}$ . Whereas, there was a change in  $-\text{OH}$  stretching of encapsulated wall material and peaks shifted higher wavelength such as  $3295\text{ cm}^{-1}$ . It was noticed that when walnut oil was encapsulated in whey protein and gum arabic mixture, a further shift of peak was noticed. The peak shifted to higher wavelength of  $3312\text{ cm}^{-1}$ . Thus, the peak shift was assigned to the presence of hydroxyl and amino stretching and confirmed the hydrogen bonding involved in interaction between gum arabic and whey protein.<sup>41</sup> It confirmed that walnut oil efficiently encapsulated in the core area of the mixtures, which was further strengthened by wall material. Besides, the  $\text{C}-\text{H}$  stretch vibration of  $-\text{CH}_3$  ( $2922\text{ cm}^{-1}$ ) significantly moved to increased wavelength ( $2933\text{ cm}^{-1}$ ) during encapsulation of walnut oil. It stated that the possible hydrogen interaction occurred between the hydrogen of  $-\text{OH}$  or  $-\text{CH}_3$  of the whey protein and gum arabic and the oxygen of the hydroxyl group of walnut oil. The spectrum of encapsulated walnut oil within wall material revealed a strong bond at  $1059\text{ cm}^{-1}$  that is related to stretching of  $\text{C}=\text{O}$  and indicates the complex formation between biopolymers. Moreover, the absorbance peaks of asymmetric stretching vibration of  $-\text{COOH}$  ( $1643\text{ cm}^{-1}$ ) groups and methylene bend ( $1403\text{ cm}^{-1}$ ) appeared after walnut oil encapsulation, and the vibration peak at about  $1744\text{ cm}^{-1}$  in walnut oil disappeared because of the  $\text{C}-\text{C}$  stretching bond. This confirmed that walnut oil encapsulated in whey protein and gum arabic mixture. Similar results were also found when nanoencapsulated fish oil within Persian gum–chitosan material was studied for its secondary structure.<sup>42</sup>

Differential scanning calorimetry (DSC) was employed to assess the thermodynamic characteristics of the optimized WON. This involved estimating the heat absorbed or discharged during the temperature control system. It is imperative to note that the outcomes derived from this study were qualitative in nature. Figure 5 shows the variations in DSC curves of the optimized WON in relation to the temperature. In the context of DSC measurements, the detection of the endothermic peak in the thermal scrutiny spectrum indicates that the peak is situated within the temperature range associated with the thermal denaturation

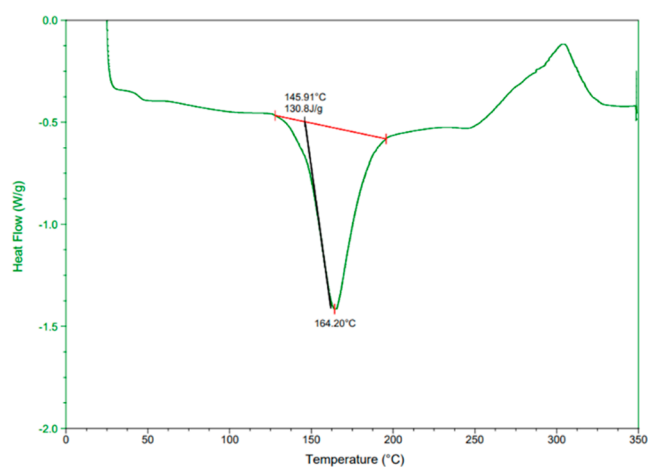


**Figure 5.** Thermal analytical study profile of optimized walnut oil nanoparticles.

of the sample. The specific heat at which this peak occurs serves as a representation of the thermal denaturation temperature for the sample. It is noteworthy that a higher denaturation temperature signifies enhanced thermal stability of the sample.<sup>27,43</sup> Figure 5 indicates the peak of the embedded walnut oil nanoparticles, corresponding to the denaturation temperature zone.

The curve represents the rise in denaturation temperature of WON along with a sharp characteristic peak at  $164.20\text{ }^\circ\text{C}$ . These findings are consistent with a study where nanocapsules of composite essential oil from cinnamon–thyme–ginger demonstrated a higher denaturation temperature ( $160\text{ }^\circ\text{C}$ ) compared to composite essential oil alone, which exhibited a denaturation temperature of  $106\text{ }^\circ\text{C}$ .<sup>39</sup> The results suggest that the formulated walnut oil within the coating material (gum arabic–whey protein) as a nanocapsule has a protective barrier and exhibits positive heat stability. The elevated denaturation heating range of gum arabic and whey protein could be associated with the molecular relationship between the protein and polysaccharides. Certainly, previous research has demonstrated that the interaction between proteins and polysaccharides has the potential to enhance the heat stability of protein–polysaccharide formulations. Polysaccharides contribute to improved heat resistance through intermolecular interactions, for instance, hydrophobic interactions.<sup>19</sup> Additionally, these observations are consistent with a study by Zhou, Pan, Ye, Jia, Ma, and Ge,<sup>44</sup> which highlighted soybean protein isolate and maltodextrin as effective protective agents for walnut oil. These compounds were shown to form a defense system against both oxidation and heat.

**3.4. Antioxidant Activity.** To determine the radical trapping capacity of WON, the antioxidant capacity was measured using DPPH. Nanoencapsulation is renowned for its capability to augment the antioxidant capabilities of natural molecules. Consequently, the scavenging activity of the WON on DPPH radicals was evaluated to gauge its free radical–radical-scavenging prowess. As illustrated in Figure 6, WON displayed a remarkable inhibition of 96% at a concentration of  $100\text{ }\mu\text{g/mL}$ . In contrast, walnut oil at a similar concentration exhibited a lower inhibition of 40%. These results align with a prior study that showed clove oil nanoparticle formation inhibited oxidation.<sup>45</sup>

**3.5. Microstructural Analysis.** SEM images in Figure 7 show the morphology and size of WON achieved through

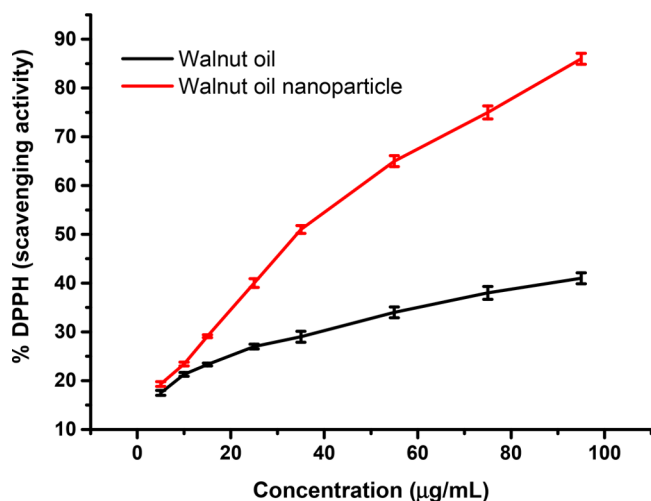


**Figure 6.** Antioxidant activities of walnut oil and walnut oil nanoparticles

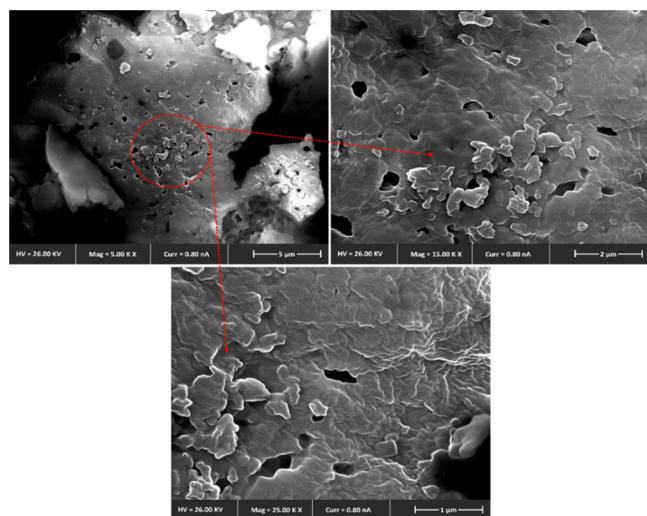


**Figure 7.** Scanning electron micrographs (SEM) of the walnut oil loaded nanoparticles.

freeze-drying when the surfactant mixture, walnut oil, and sonication time were 49.50%, 15%, and 180 s, respectively. The particle morphology analysis indicates that the matrix surface is notably smooth and fragile, characterized by a porous structure.<sup>46,47</sup> The detected porosity is likely due to the formation of pores, which can be attributed to the presence of either ice crystals or air bubbles throughout the freezing step. In this process, the liquid samples undergo initial freezing, followed by subsequent water evaporation via sublimation. This process significantly contributes to the development of porous structures. Additionally, the presence of numerous pores can be attributed to mechanical stresses induced through inhomogeneous drying at various positions within the feed mixture, particularly during the initial stages of the drying process. Figure 7 depicts the homogeneous dispersion of nanosized gum arabic-whey protein complex particles throughout the matrix, aligning well with the particle size results obtained from DLS. Specifically, it was discovered that the average size of the WON obtained from treatment 8 is approximately 80 nm.

The inclusion of protein materials in the system has a significant impact on the interactions. Specifically, the altered conformation of the protein when interacting with other materials leads to more valuable outcomes. These interactions provide the stabilization of the complex through electrostatic forces and a reduction in the overall surface tension of systems.<sup>48</sup> Similar findings were noted in research where positively charged chitosan and negatively charged whey protein facilitated the embedding of the ergosterol-enriched extract. This interaction led to complex aggregation, ultimately resulting in the development of constant microcapsules.<sup>49</sup> The obtained result aligns with findings reported in a study focused on nanoparticle preparation using chitosan and whey protein.<sup>46</sup> Particle accumulation may be attributed to a high amount of chitosan and the relatively small size of the microcapsules, while the diminutive size of the microcapsules has the potential to reduce the repulsive forces between molecules.<sup>50,51</sup>

#### 4. CONCLUSION

This study highlighted the influence of the gum arabic–whey protein on the WON. WON was synthesized using gum arabic and whey protein, and RSM was applied to optimize the particle size, PDI, moisture, and EE of the encapsulated samples. The results revealed the coating material properties of gum arabic–whey protein complexes. The obtained WON of 84 nm displayed an increased encapsulation efficiency. Structural and thermal studies exhibited the stability of walnut oil in these complexes. Antioxidant activity was higher in the WON with an increasing concentration. The morphology of the samples (WON) revealed that the surface of the matrix was relatively smooth and fragile with a porous structure. Thus, this study confirmed walnut oil's excellent optimization and encapsulation into the gum arabic and whey protein complexes.

#### AUTHOR INFORMATION

##### Corresponding Authors

**Gebremichael Gebremedhin Hailu** – Department of Food Technology and Process Engineering, Oda Bultum University, Asebe Teferi 0000, Ethiopia; [orcid.org/0000-0002-7376-0700](https://orcid.org/0000-0002-7376-0700); Email: [mikialejr@gmail.com](mailto:mikialejr@gmail.com)

**Rabia Shabir Ahmad** – Department of Food Science, Faculty of Life Sciences, Government College University Faisalabad, Faisalabad, Punjab 38000, Pakistan; Email: [rabiaahmad@gcuf.edu.pk](mailto:rabiaahmad@gcuf.edu.pk)

##### Authors

**Ali Tahir** – Department of Food Science, Faculty of Life Sciences, Government College University Faisalabad, Faisalabad, Punjab 38000, Pakistan; Biological Systems Engineering, Washington State University, Pullman, Washington 99164, United States

**Muhammad Kamran Khan** – Department of Food Science, Faculty of Life Sciences, Government College University Faisalabad, Faisalabad, Punjab 38000, Pakistan

**Muhammad Imran** – Department of Food Science, Faculty of Life Sciences, Government College University Faisalabad, Faisalabad, Punjab 38000, Pakistan

Complete contact information is available at:

<https://pubs.acs.org/10.1021/acsomega.4c01141>

## Author Contributions

Conceptualization, R.S.A. and G.G.H.; methodology, A.T. and M.I.; software and validation, M.K.K.; formal analysis, A.T.; writing—original draft preparation, A.T.; writing—review and editing, R.S.A. and G.G.H.; and supervision, R.S.A. All authors have read and agreed to the published version of the manuscript.

## Funding

This research did not receive any specific grant from funding agencies in the public, commercial, or not-for-profit sector.

## Notes

The authors declare no competing financial interest.

## ACKNOWLEDGMENTS

The authors are thankful for the financial support of the Higher Education Commission, Pakistan under the slot of International Research Support Initiative Program (IRSIP). The authors acknowledged the guidance and facilities provided by Prof. Dr. Shyam Sablani, Biological System Engineering, Washington State University.

## REFERENCES

- (1) Shamaei, S.; Seiedlou, S. S.; Aghbashlo, M.; Tsotsas, E.; Kharaghani, A. Microencapsulation of walnut oil by spray drying: Effects of wall material and drying conditions on physicochemical properties of microcapsules. *Inno. Food Sci. Emerg. Technol.* **2017**, *39*, 101–112.
- (2) Gao, P.; Liu, R.; Jin, Q.; Wang, X. Effects of processing methods on the chemical composition and antioxidant capacity of walnut (*Juglans regia* L.) oil. *LWT* **2021**, *135*, 109958.
- (3) Homayoonfal, M.; Khodaiyan, F.; Mousavi, S. M. Optimization of walnut oil nanoemulsions prepared using ultrasonic emulsification: A response surface method. *J. Dispers. Sci. Technol.* **2014**, *35* (5), 685–694.
- (4) Kergomard, J.; Paboeuf, G.; Barouh, N.; Villeneuve, P.; Schafer, O.; Wooster, T. J.; Bourlieur, C.; Vié, V. Stability to oxidation and interfacial behavior at the air/water interface of minimally-processed versus processed walnut oil-bodies. *Food Chem.* **2021**, *360*, 129880.
- (5) Tabatabaei, M.; Rajaei, A.; Hosseini, E.; Aghbashlo, M.; Gupta, V. K.; Lam, S. S. Effect of type of fatty acid attached to chitosan on walnut oil-in-water Pickering emulsion properties. *Carbohydr. Polym.* **2022**, *291*, 119566.
- (6) Tian, L.; Zhang, S.; Yi, J.; Zhu, Z.; Decker, E. A.; McClements, D. J. The impact of konjac glucomannan on the physical and chemical stability of walnut oil-in-water emulsions coated by whey proteins. *J. Sci. Food Agric.* **2022**, *102* (10), 4003–4011.
- (7) Zhang, L.; Wu, S.; Jin, X. Fatty acid stable carbon isotope ratios combined with oxidation kinetics for characterization and authentication of walnut oils. *J. Agric. Food Chem.* **2021**, *69* (23), 6701–6709.
- (8) Bustamante, M.; Mitcham, E. Impact of low oxygen storage on post-storage quality of pasteurized walnut (*Juglans regia* L.) kernels. *Postharvest Biol. Technol.* **2023**, *205*, 112542.
- (9) Pateiro, M.; Gómez, B.; Muneke, P. E.; Barba, F. J.; Putnik, P.; Kovačević, D. B.; Lorenzo, J. M. Nanoencapsulation of promising bioactive compounds to improve their absorption, stability, functionality and the appearance of the final food products. *Molecules* **2021**, *26* (6), 1547.
- (10) Mirzaei-Mohkam, A.; Garavand, F.; Dehnad, D.; Keramat, J.; Nasirpour, A. Optimisation, antioxidant attributes, stability and release behaviour of carboxymethyl cellulose films incorporated with nanoencapsulated vitamin E. *Prog. Org. Coat.* **2019**, *134*, 333–341.
- (11) Khan, W. A.; Butt, M. S.; Pasha, I.; Jamil, A. Microencapsulation of vitamin D in protein matrices: In vitro release and storage stability. *J. Food Meas. Charact.* **2020**, *14*, 1172–1182.
- (12) Khan, W. A.; Butt, M. S.; Pasha, I.; Saeed, M.; Yasmin, I.; Ali, M.; Azam, M.; Khan, M. S. Bioavailability, rheology, and sensory

evaluation of mayonnaise fortified with vitamin D encapsulated in protein-based carriers. *J. Texture Stud.* **2020**, *51* (6), 955–967.

- (13) Moghadam, F. V.; Pourahmad, R.; Mortazavi, A.; Davoodi, D.; Azizinezhad, R. Use of fish oil nanoencapsulated with gum arabic carrier in low fat probiotic fermented milk. *Food Sci. Anim. Resour.* **2019**, *39* (2), 309.

- (14) Vahidmoghadam, F.; Pourahmad, R.; Mortazavi, A.; Davoodi, D.; Azizinezhad, R. Characteristics of freeze-dried nanoencapsulated fish oil with whey protein concentrate and gum arabic as wall materials. *Food Sci. Technol.* **2019**, *39*, 475–481.

- (15) Ribeiro, E. F.; Morell, P.; Nicoletti, V. R.; Quiles, A.; Hernando, I. Protein and polysaccharide-based particles used for Pickering emulsion stabilisation. *Food Hydrocoll.* **2021**, *119*, 106839.

- (16) Yolmeh, M.; Jafari, S. M. Applications of response surface methodology in the food industry processes. *Food Bioproc. Technol.* **2017**, *10* (3), 413–433.

- (17) Wang, C. N.; Nguyen, N. A. T.; Dang, T. T. Solving order planning problem using a heuristic approach: The case in a building material distributor. *Appl. Sci.* **2020**, *10* (24), 8959.

- (18) Saravana, P. S.; Shanmugapriya, K.; Gereniu, C. R. N.; Chae, S. J.; Kang, H. W.; Woo, H. C.; Chun, B. S. Ultrasound-mediated fucoxanthin rich oil nanoemulsions stabilized by  $\kappa$ -carrageenan: Process optimization, bio-accessibility and cytotoxicity. *Ultrason. Sonochem.* **2019**, *55*, 105–116.

- (19) Yang, Z.; He, Q.; Ismail, B. B.; Hu, Y.; Guo, M. Ultrasonication induced nano-emulsification of thyme essential oil: Optimization and antibacterial mechanism against *Escherichia coli*. *Food Control* **2022**, *133*, 108609.

- (20) Esfahani, R.; Jafari, S. M.; Jafarpour, A.; Dehnad, D. Loading of fish oil into nanocarriers prepared through gelatin-gum arabic complexation. *Food Hydrocoll.* **2019**, *90*, 291–298.

- (21) Ali, A.; Ali, S.; Aqil, M.; Imam, S. S.; Ahad, A.; Qadir, A. Thymoquinone loaded dermal lipid nano particles: box Behnken design optimization to preclinical psoriasis assessment. *J. Drug Delivery Sci. Technol.* **2019**, *52*, 713–721.

- (22) Kapoor, H.; Aqil, M.; Imam, S. S.; Sultana, Y.; Ali, A. Formulation of amlodipine nano lipid carrier: formulation design, physicochemical and transdermal absorption investigation. *J. Drug Delivery Sci. Technol.* **2019**, *49*, 209–218.

- (23) Moolakkadath, T.; Aqil, M.; Ahad, A.; Imam, S. S.; Iqbal, B.; Sultana, Y.; Mujeeb, M.; Iqbal, Z. Development of transethosomes formulation for dermal fisetin delivery: Box–Behnken design, optimization, in vitro skin penetration, vesicles–skin interaction and dermatokinetic studies. *Artif. Cells Nanomed. Biotechnol.* **2018**, *46* (sup2), 755–765.

- (24) Sharma, O. P.; Bhat, T. K. DPPH antioxidant assay revisited. *Food Chem.* **2009**, *113* (4), 1202–1205.

- (25) Hasanvand, E.; Fathi, M.; Bassiri, A.; Javanmard, M.; Abbaszadeh, R. Novel starch based nanocarrier for vitamin D fortification of milk: Production and characterization. *Food Bioprod. Process.* **2015**, *96*, 264–277.

- (26) Ovissipour, M.; Rasco, B.; Tang, J.; Sablani, S. Kinetics of protein degradation and physical changes in thermally processed Atlantic salmon (*Salmo salar*). *Food Bioproc. Technol.* **2017**, *10*, 1865–1882.

- (27) Yang, K.; Liu, A.; Hu, A.; Li, J.; Zen, Z.; Liu, Y.; Tang, S.; Li, C. Preparation and characterization of cinnamon essential oil nano-capsules and comparison of volatile components and antibacterial ability of cinnamon essential oil before and after encapsulation. *Food Control* **2021**, *123*, 107783.

- (28) Kumari, M.; Gupta, S. K. Response surface methodological (RSM) approach for optimizing the removal of trihalomethanes (THMs) and its precursor's by surfactant modified magnetic nano-adsorbents (sMNP)-An endeavor to diminish probable cancer risk. *Sci. Rep.* **2019**, *9* (1), 18339.

- (29) Alara, O. R.; Abdurahman, N. H.; Olalere, O. A. Optimization of microwave-assisted extraction of flavonoids and antioxidants from *Vernonia amygdalina* leaf using response surface methodology. *Food Bioprod. Process.* **2018**, *107*, 36–48.

- (30) Azizanbari, C.; Ghanbarzadeh, B.; Hamishehkar, H.; Hosseini, M. Gellan-Caseinate nanocomplexes as a carrier of Omega-3 fatty acids: Study of particle size, Rheological properties and Encapsulation efficiency. *J. Food Process. Preserv.* **2013**, *5* (2), 19–42.
- (31) Sarheed, O.; Dibi, M.; Ramesh, K. V. Studies on the effect of oil and surfactant on the formation of alginate-based O/W lidocaine nanocarriers using nanoemulsion template. *Pharmaceutics* **2020**, *12* (12), 1223.
- (32) Marhamati, M.; Ranjbar, G.; Rezaie, M. Effects of emulsifiers on the physicochemical stability of Oil-in-water Nanoemulsions: A critical review. *J. Mol. Liq.* **2021**, *340*, 117218.
- (33) Masarudin, M. J.; Cutts, S. M.; Evison, B. J.; Phillips, D. R.; Pigram, P. J. Factors determining the stability, size distribution, and cellular accumulation of small, monodisperse chitosan nanoparticles as candidate vectors for anticancer drug delivery: application to the passive encapsulation of [14C]-doxorubicin. *Nanotechnol. Sci. Appl.* **2015**, 67–80.
- (34) Stoylov, S. P. Stable colloids at the isoelectric point: Dipolar vs. electrostatic interactions. *Colloids Surf. A Physicochem. Eng. Asp.* **2014**, *460*, 516–518.
- (35) Rashid, R.; Masoodi, F. A.; Wani, S. M.; Manzoor, S.; Gull, A. Ultrasound assisted extraction of bioactive compounds from pomegranate peel, their nanoencapsulation and application for improvement in shelf life extension of edible oils. *Food Chem.* **2022**, *385*, 132608.
- (36) Anwar, S. H.; Kunz, B. The influence of drying methods on the stabilization of fish oil microcapsules: Comparison of spray granulation, spray drying, and freeze drying. *J. Food Eng.* **2011**, *105* (2), 367–378.
- (37) Ghasemi, S.; Jafari, S. M.; Assadpour, E.; Khomeiri, M. Production of pectin-whey protein nano-complexes as carriers of orange peel oil. *Carbohydr. Polym.* **2017**, *177*, 369–377.
- (38) Saberi, M.; Hashemiravan, M.; Farhadyar, N. Influence of Casein and Inulin on the properties of nano-particle encapsulation of fish oil. *J. Bio. Env. Sci.* **2014**, *4* (2), 318–326.
- (39) Hu, J.; Zhang, Y.; Xiao, Z.; Wang, X. Preparation and properties of cinnamon-thyme-ginger composite essential oil nanocapsules. *Ind. Crops Prod.* **2018**, *122*, 85–92.
- (40) Gómez-Mejía, E.; Rosales-Conrado, N.; León-González, M. E.; Madrid, Y. Citrus peels waste as a source of value-added compounds: Extraction and quantification of bioactive polyphenols. *Food Chem.* **2019**, *295*, 289–299.
- (41) Fan, L. F.; Rong, M. Z.; Zhang, M. Q.; Chen, X. D. A very simple strategy for preparing external stress-free two-way shape memory polymers by making use of hydrogen bonds. *Macromol. Rapid Commun.* **2018**, *39* (12), 1700714.
- (42) Raeisi, S.; Ojagh, S. M.; Quek, S. Y.; Pourashouri, P.; Salaiin, F. Nano-encapsulation of fish oil and garlic essential oil by a novel composition of wall material: Persian gum-chitosan. *LWT* **2019**, *116*, 108494.
- (43) Bowers, K.; Markova, N. Value of DSC in characterization and optimization of protein stability. *Methods Mol. Biol.* **2019**, *1964*, 33–44.
- (44) Zhou, D.; Pan, Y.; Ye, J.; Jia, J.; Ma, J.; Ge, F. Preparation of walnut oil microcapsules employing soybean protein isolate and maltodextrin with enhanced oxidation stability of walnut oil. *LWT* **2017**, *83*, 292–297.
- (45) Mahdi, A. A.; Al-Maqtari, Q. A.; Mohammed, J. K.; Al-Ansi, W.; Cui, H.; Lin, L. Enhancement of antioxidant activity, antifungal activity, and oxidation stability of Citrus reticulata essential oil nanocapsules by clove and cinnamon essential oils. *Food Biosci.* **2021**, *43*, 101226.
- (46) De Queiroz, J. L. C.; De Araújo Costa, R. O.; Rodrigues Matias, L. L.; De Medeiros, A. F.; Teixeira Gomes, A. F.; Santos Pais, T. D.; Passos, T. S.; Maciel, B. L. L.; Dos Santos, E. A.; De Araújo Morais, A. H. Chitosan-whey protein nanoparticles improve encapsulation efficiency and stability of a trypsin inhibitor isolated from Tamarindus indica L. *Food Hydrocoll.* **2018**, *84*, 247–256.
- (47) Muhoza, B.; Xia, S.; Cai, J.; Zhang, X.; Duhoranimana, E.; Su, J. Gelatin and pectin complex coacervates as carriers for cinnamaldehyde: Effect of pectin esterification degree on coacervate formation, and enhanced thermal stability. *Food Hydrocoll.* **2019**, *87*, 712–722.
- (48) Bouyer, E.; Mekhloufi, G.; Rosilio, V.; Grossiord, J. L.; Agnely, F. Proteins, polysaccharides, and their complexes used as stabilizers for emulsions: Alternatives to synthetic surfactants in the pharmaceutical field? *Int. j. Pharm.* **2012**, *436* (1–2), 359–378.
- (49) Rudke, A. R.; Heleno, S. A.; Fernandes, I. P.; Prieto, M. A.; Gonçalves, O. H.; Rodrigues, A. E.; Ferreira, I. C. F. R.; Barreiro, M. F. Microencapsulation of ergosterol and Agaricus bisporus L. extracts by complex coacervation using whey protein and chitosan: Optimization study using response surface methodology. *LWT* **2019**, *103*, 228–237.
- (50) Joye, I. J.; McClements, D. J. Production of nanoparticles by anti-solvent precipitation for use in food systems. *Trends Food Sci. Technol.* **2013**, *34* (2), 109–123.
- (51) Ahmed, K. F.; Aschi, A.; Nicolai, T. Formation and characterization of chitosan-protein particles with fractal whey protein aggregates. *Colloids Surf., B* **2018**, *169*, 257–264.